ELSEVIER

Biochimica et Biophysica Acta 1463 (2000) 355–373

BIOCHIMICA ET BIOPHYSICA ACTA
BBA

www.elsevier.com/locate/bba

Nucleotide chain length and the morphology of complexes with cationic amphiphiles: ^{31}P-NMR observations

Peter Mitrakos, Peter M. Macdonald *

Department of Chemistry, University of Toronto at Mississauga, 3359 Mississauga Road, Mississauga, ON L5L 1C6, Canada

Received 24 May 1999; received in revised form 11 November 1999; accepted 11 November 1999

Abstract

^{31}P-NMR and UV spectroscopies were used to study the interactions between cationic amphiphile-containing lipid bilayers and either a phosphorothioate oligonucleotide (OligoS) ($n=21$) or polyadenylic acid (PolyA) ($n\approx18\,000$). Multilamellar vesicles (MLVs) were composed of 1-palmitoyl-2-oleoyl-*sn*-glycero-3-phosphocholine (POPC) or 1,2-dioleoyl-*sn*-glycero-3-phosphoethanolamine (DOPE) in binary mixture with either of the cationic lipids, *N*-[1-(2,3-dioleoyloxy)propyl]-*N*′,*N*′,*N*′-trimethylammonium chloride (DOTAP) or cetyltrimethylammonium bromide (CTAB). A UV-difference assay showed that OligoS binding ceased above a 1:1 anion/cation ratio, while PolyA binding continued until a 2:1 ratio was reached, indicating a 'flat' conformation for bound OligoS, but not necessarily for PolyA. Cross-polarization ^{31}P-NMR of the nucleotide chains bound to 100% DOTAP MLVs produced spectra virtually identical to those of dry powders of OligoS or PolyA, indicating effective immobilization of the surface-bound nucleotide chains. Hahn echo ^{31}P-NMR showed that MLVs composed of binary mixtures of POPC with DOTAP or CTAB retained a lamellar bilayer architecture upon adding nucleotide chains. At less than stoichiometric anion/cation ratios little or no signal attributable to free nucleotide chains was visible. A narrow signal at the chemical shift expected for phosphorothiodiesters or phosphodiesters became visible at greater levels of added OligoS or PolyA, respectively, indicating the presence of mobile nucleotide chains. Salt addition caused complete desorption of the nucleotide chains. When POPC was replaced with DOPE, binding of OligoS or PolyA produced non-bilayer lipid phases in the presence of DOTAP, but not in the presence of CTAB.

Keywords: Cationic amphiphile; Polynucleotide; Molecular weight; ^{31}P-Nuclear magnetic resonance; Phosphatidylethanolamine; Phosphatidylcholine; Ionic strength

1. Introduction

DNA packaged with cationic liposomes can successfully transfer into a cell's interior via an endocytotic mechanism [1–3]. Once endocytosed, some stimulus causes destabilization of the endosomal membrane and release of the naked genetic material for uptake by the cell's transcription mechanism. The detailed morphology of the DNA+amphiphile 'pack-

Abbreviations: ^{31}P, phosphorus 31; ^{2}H, deuterium; NMR, nuclear magnetic resonance; PolyA, polyadenylic acid; OligoS, phosphorothioate oligonucleotide; DOTAP, *N*-(1-(2,3-dioleoyloxy)propyl)-*N*,*N*,*N*-trimethylammonium chloride; CTAB, cetyltrimethylammonium bromide; POPC, 1-palmitoyl-2-oleoyl-*sn*-glycero-3-phosphocholine; DOPE, 1,2-dioleoyl-*sn*-glycero-3-phosphoethanolamine; MLV, multilamellar vesicles; H_{II}, hexagonal; Q_{II}, cubic; L_α, lamellar

* Corresponding author. Fax: (905) 8285425;
E-mail: pmacdona@credit.erin.utoronto.ca

0005-2736/00/$ – see front matter
PII: S0005-2736(99)00232-1

age' is expected to be a major factor determining the efficiency of transmembrane transfer of genetic material. The structure of the complexes depends on various factors such as the size of the DNA, the size of the liposomes, the identity of the cationic amphiphile, and the nature of any added 'helper' lipids [4–12].

The latter are often those which induce non-lamellar architectures in lipid assemblies. For instance, studies comparing phosphatidylcholine (PC), a bilayer stabilizing amphiphile, with phosphatidylethanolamine (PE), a bilayer destabilizing amphiphile, indicate that in binary mixtures with cationic amphiphiles PE produces an enhancement of the potency of gene transfer, at least in vitro [13,14]. It is hypothesized that non-lamellar architectures produce a more potent transfection package by locally destabilizing the target membrane's lipid bilayer, thereby lowering the energy barrier to transmembrane transport of the polynucleic acid [5,9].

It is also recognized that different cationic amphiphiles display different transfection efficiencies [15–17]. However, a given cationic amphiphile is not necessarily the most efficient agent of transfection for all cell types. The role of the cationic lipid is to electrostatically (and reversibly) bind both DNA and the target membrane. However, it might also influence the resulting morphology of the package, thereby either assisting or resisting the 'helper' lipids. Here the details have yet to be established.

As to the role played by DNA, it has been shown that the efficiency of DNA entrapment [18] and the transfection potency [19] decrease with higher molecular weight DNA fragments. Various morphologies of the 'packaged' DNA have been reported, including lamellar and hexagonal arrangements [20,21], depending on the details of the amphiphile composition. Clearly, the interactions between the DNA, the cationic amphiphile, and any helper lipid all contribute to the final morphology of the complex. At present, these interactions remain poorly understood.

We report here ^{31}P-NMR spectroscopic studies of the morphology of complexes formed by mixing nucleotide chains with cationic amphiphiles and helper lipids. To examine the influence of nucleotide chain length, we compare two different single chain species, one an oligomer of 21 nucleotides and the other a polymer approx. 18 000 nucleotides in length. To observe the effects of cationic amphiphile structure, we alternate between two different cationic amphiphiles, one a single chain and the other a double chain species. To clarify the role of the helper lipid, we incorporate two different zwitterionic phospholipids, one being PC and the other PE.

The ^{31}P-NMR spectra permit one to observe the architecture of the phospholipid self-assembly and the dynamics of the nucleotide chains, independently and simultaneously. Thus, one may study how the nucleotide chains, the cationic amphiphile, and the helper lipid, interact to produce either bilayer or non-bilayer morphologies. In addition, one may examine the effects of complexation on nucleotide chain dynamics, and the influence thereupon of major variables such as the global anion/cation ratio and the ionic strength.

2. Materials and methods

2.1. Materials

POPC (1-palmitoyl-2-oleoyl-*sn*-glycero-3-phosphocholine), DOPE (1,2-dioleoyl-*sn*-glycero-3-phosphoethanolamine) and DOTAP (*N*-(1-(2,3-dioleoyloxy)-propyl)-*N*,*N*,*N*-trimethylammonium chloride) were purchased from Avanti Polar Lipids (Alabaster, AL). DOTAP-γ-d_9 was synthesized as described by Mitrakos and Macdonald [22]. CTAB (cetyltrimethylammonium bromide) was purchased from BDH (Toronto, ON). PolyA (polyadenylic acid, MW $\approx$ 7 000 000, $n \approx 18\,000$) was purchased from Sigma (St. Louis, MO). OligoS, a phosphorothioate oligonucleotide, 5′-GCCGAGGTCCATGTCGTAC-GC-3′ (MW 7183, $n = 21$), was a gift from ISIS Pharmaceuticals (Carlsbad, CA). The structures of these various chemical species are shown in Fig. 1.

2.2. Preparation of multilamellar vesicles

Multilamellar vesicles (MLVs) consisting of lipid mixtures of a desired composition were prepared by combining appropriate volumes of chloroform stock solutions of either DOTAP or CTAB with either POPC or DOPE. Typically the lipid mixtures consisted of 15 mg of phospholipid plus the desired

amount of either of the cationic amphiphiles. The solvent was removed under a stream of argon and the mixture was dried under vacuum overnight. The dried lipids were then hydrated in 200 μl of deionized water. The hydration process consisted of gentle warming and vortexing, followed by four cycles of freeze-thaw to ensure homogeneous mixing.

2.3. Preparation of complexes of PolyA or OligoS+MLVs

Dried lipid mixtures were prepared as described above, but were hydrated by adding the desired quantity of PolyA or OligoS dissolved in deionized water plus sufficient water and/or NaCl in water, to

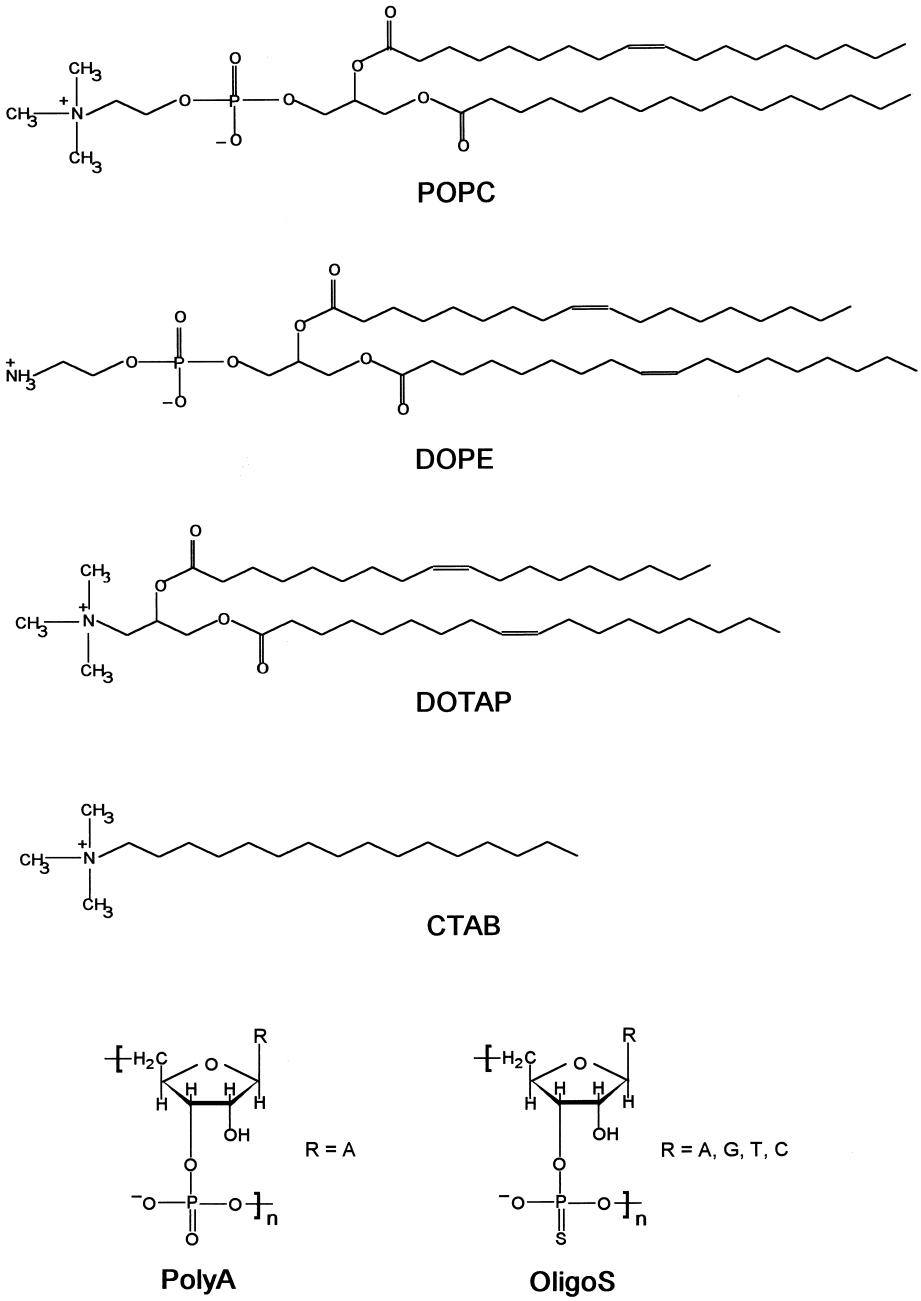

Fig. 1. Structures of the zwitterionic amphiphiles (POPC and DOPE), cationic amphiphiles (DOTAP and CTAB), and nucleic acid chains (OligoS and PolyA) employed here.

bring the final volume to 200 μl. The mixtures were once again gently warmed and vortexed and subjected to the freeze-thaw cycles.

2.4. ^{31}P-NMR spectroscopy

^{31}P-NMR spectra were recorded at room temperature on a Chemagnetics CMX300 NMR spectrometer operating at 121.25 MHz, using a Chemagnetics double-resonance magic-angle spinning (MAS) probe but without sample spinning. For hydrated MLV samples, a Hahn echo sequence with complete phase cycling of the pulses and proton decoupling during acquisition was employed as described by Rance and Byrd [23]. The 90° pulse length was 6.0 μs, the echo spacing was 30 μs, the recycle delay was 2s, the spectral width was 100 kHz, and the data size was 2K. Typically, 3600 transients were signal averaged and the free induction decay was processed with an exponential multiplication corresponding to 100 Hz line broadening prior to Fourier transformation. T_1 relaxation times were measured using a standard inversion-recovery protocol with Hahn echo detection. T_2 relaxation times were measured from the dependence of the signal intensity on the length of the delay in the Hahn echo sequence.

^{31}P-NMR spectra of dry powders of PolyA or OligoS were recorded using a single-contact cross-polarization technique combined with Hahn echo detection. In this instance the ^{1}H 90° pulse length was 4.9 μs, the contact time was 3.0 ms, the recycle delay was 5.0 s, the spectral width was 250 kHz, and the data size was 2K. Typically, 16 000 transients were signal averaged and the free induction decay was processed with an exponential multiplication corresponding to 200 Hz line broadening prior to Fourier transformation.

2.5. ^{2}H-NMR spectroscopy

^{2}H-NMR spectra were recorded on the same spectrometer operating at 45.98 MHz, using a Chemagnetics wideline deuterium probe. The quadrupolar echo sequence [24] was employed using quadrature detection with complete phase cycling of the pulse pairs, a 90° pulse width of 2.0 μs, an interpulse delay of 30 μs, a recycle delay of 100 ms, a spectral width of 50 kHz, and a 2K data size.

Typically, 6000 transients were signal averaged and the free induction decay was processed with an exponential multiplication corresponding to 100 Hz line broadening prior to Fourier transformation.

2.6. UV-difference assay of nucleotide chain-cationic amphiphile binding

Dried lipid samples were prepared as described above and sufficient PolyA or OligoS was added from separate aqueous stock solutions to achieve the desired anion:cation ratio. Further water and/or NaCl solution was added to bring the final volume of the mixture to 300 μl. The samples were then hydrated and equilibrated as described above, then centrifuged at 13 000 rpm for 1 h to pellet the lipids and bound nucleotide chains. The supernatant was decanted, diluted, and passed through a Centricon-500 microconcentrator (Amicon, Oakville, ON) to remove any unpelleted lipid. The filtrate, containing any unbound nucleotide chains, was further diluted until its UV absorbance (λ_{max} = 258 nm) fell into the concentration regime (between 3.5 and 35 μg/ml) where Beer's law was obeyed, as measured using a Hewlett Packard 8452A Diode Array spectrophotometer. The nucleotide concentration in the original supernatant was then calculated from a standard curve, and the amount bound was calculated from the difference with respect to the initial concentration.

3. Results

3.1. UV-difference assay of OligoS or PolyA binding to DOTAP/POPC mixtures

The binding of two different-sized nucleotide chains, OligoS and PolyA, to cationic MLVs composed of DOTAP/POPC (30/70) (all ratios are molar ratios) was quantified using a UV-difference assay, as described Section 2.

The results are displayed in Fig. 2 and show that the binding of either nucleotide chain is essentially quantitative up to the anion/cation equivalence point. This indicates that in this charge regime the nucleotide chains lie flat on the lipid bilayer surface,

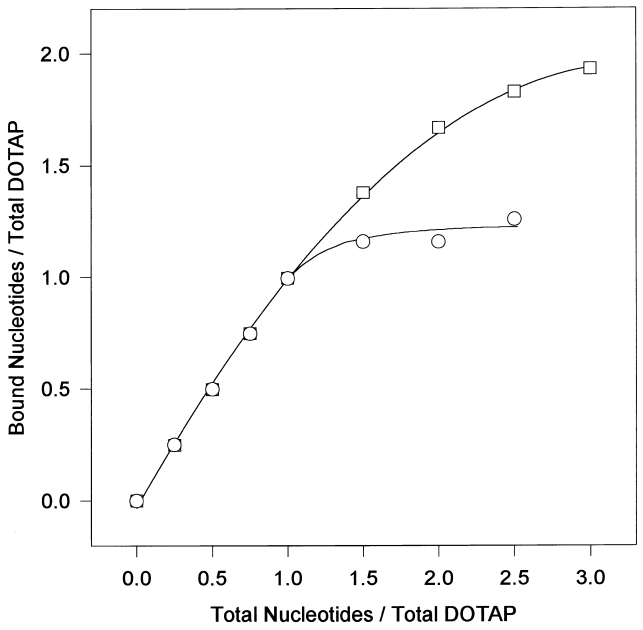

Fig. 2. UV-difference assay of OligoS (○) and PolyA (□) binding to DOTAP/POPC (30/70) mixtures. The binding is expressed in terms of the number of nucleotide anions bound per DOTAP cation, relative to the total nucleotide anions added per DOTAP cation.

as suggested previously for both polynucleotides [25–27] and synthetic polyelectrolytes [28–30].

At just slightly greater than the anion/cation equivalence point, binding of OligoS ceases. PolyA binding continues, however, until almost a 2:1 anion/cation ratio is reached. Such behavior is also observed with a variety of large synthetic polyelectrolytes (approx. 300–500 monomer units) [30]. It indicates that PolyA is able to bind to the lipid bilayer surface when only a fraction of its potential attachments sites are in actual contact with the surface. Consequently, the nucleotide segment density profile of the bound PolyA must extend outwards significantly from the surface. Thus, PolyA must undergo a change from a 'pancake' conformation below the equivalence point, to one reminiscent of a 'brush' above the equivalence point. In the case of OligoS, the 'flat' conformation persists both below and above the equivalence point.

3.2. ^{31}P-NMR of complexes of OligoS or PolyA with 100% DOTAP

Fig. 3 shows various ^{31}P-NMR spectra of OligoS (left hand column) and PolyA (right hand column) obtained using the cross-polarization technique described in Section 2. The lower spectra originated from dry powders of the respective nucleotide chains. The spectral line shapes are characteristic of static phosphorothio- and phosphodiesters, respectively. The isotropic chemical shifts, static chemical shift tensor components, and asymmetry parameters are listed in Table 1.

The middle spectra in Fig. 3 were obtained with OligoS or PolyA bound to 100% DOTAP MLVs in a ratio of 0.5 phosphorus anions per DOTAP cationic charge. The excess of cationic charge ensures that the nucleotide chains are complexed quantitatively. Since there are no phospholipids in these mixtures, the ^{31}P-NMR signal originates solely with the nucleotide chains. The resulting spectra are similar, if not identical, to those of the corresponding

Table 1
^{31}P-NMR isotropic chemical shifts and anisotropic chemical shift tensor elements for OligoS and PolyA as dry powders or bound to hydrated 100% DOTAP

Nucleotide/DOTAP	δ_0	σ_{11}	σ_{22}	σ_{33}	$\sigma_{33}-\sigma_{11}$	η
OligoS						
Dry powder	56	136	98	−68	204	0.31
0.5:1	56	128	82	−35	163	0.51
1:1	56	125	80	−40	163	0.47
PolyA						
Dry powder	0	96	31	−115	211	0.56
0.5:1	0	81	20	−105	186	0.58
1:1	0	63	0	−92	155	0.68

All chemical shifts are in parts per million (ppm) referenced to 85% H_3PO_4. Anisotropic chemical shift tensor elements are defined such that $|\sigma_{33}| > |\sigma_{22}| > |\sigma_{11}|$ where $\sigma_{ii} = (\delta_{ii} - \delta_0)$ and δ_0 and δ_{ii} are the observed isotropic and anisotropic chemical shifts. The asymmetry parameter is defined as $\eta = (\sigma_{22} - \sigma_{11})/\sigma_{33}$.

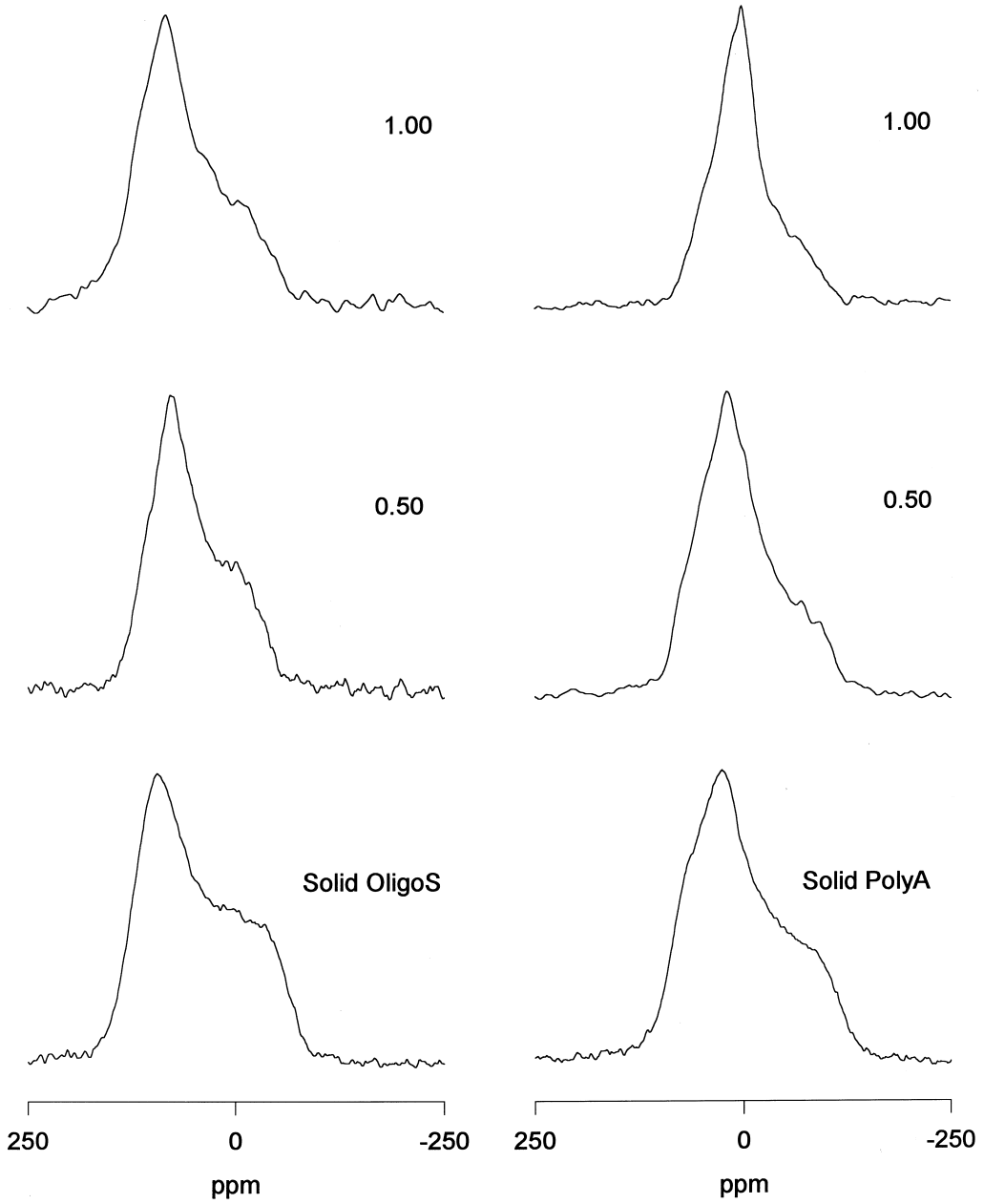

Fig. 3. Cross-polarization ^{31}P-NMR spectra of OligoS (left hand column) and PolyA (right hand column) in the form of a dry powder (bottom spectra), mixed with fully hydrated 100% DOTAP in an anion/cation charge ratio of 0.5:1 (middle spectra), or mixed with fully hydrated 100% DOTAP in an anion/cation charge ratio of 1:1 (top spectra). The isotropic chemical shifts, chemical shift tensor components and asymmetry parameters for the various spectra are listed in Table 1.

dry powders. Therefore, the bound nucleotide chains are largely immobilized under these circumstances as a result of their Coulombic attraction to, and charge pairing with, the oppositely charged amphiphiles. Nevertheless, there is a significant decrease in the overall chemical shift anisotropy for the bound nucleotide chains, as detailed in Table 1. This suggests the presence of local limited-amplitude segmental librations within the bound nucleotide chain. One must interpret such effects with caution, however, since ion pairing can alter the electron charge density distribution at the phosphorus atom, and this

effect would be manifest in the values of the chemical shift tensor components. Detailed relaxation time studies would be useful in resolving these possibilities.

The top spectra in Fig. 3 were obtained when OligoS or PolyA was added to 100% DOTAP MLVs in a 1:1 ratio of anionic to cationic charge. Overall, these spectra are again indicative of immobilization of the nucleotide chains at the lipid bilayer surface. For OligoS, the spectra at 0.5:1 and 1:1 charge ratios are similar, but the quality of the spectra limits further analysis, given their signal-to-noise ratios. However, for PolyA at this anion/cation ratio there is obviously a further narrowing of the chemical shift anisotropy, with a clear shift of the highest intensity spectral feature towards the isotropic chemical shift position of PolyA. Thus, at the charge equivalence point PolyA enjoys greater motional freedom than OligoS. In the absence of more detailed studies it is impossible to decide whether such spectra represent a superposition of populations with slightly different mobilities, or a single population with a single average mobility. Regardless, it is likely that PolyA is prevented from lying flat on the 100% DOTAP surface due to its size and the consequent entanglement effects, and that this is the origin of its greater mobility relative to OligoS.

3.3. ^{2}H-NMR of DOTAP-γ-d_9 in complexes of OligoS or PolyA with 100% DOTAP

Fig. 4 shows a series of ^{2}H-NMR spectra of 100% DOTAP-γ-d_9 in complexes with either OligoS (left hand column) or PolyA (right hand column). The top spectrum in each column is identical and was obtained in the absence of nucleotide chains. One sees the typical Pake doublet line shape expected for deuterons experiencing anisotropic rotational averaging, such as one anticipates for lipids in a liquid-crystalline lamellar bilayer environment. The value of the quadrupolar splitting, corresponding to the separation in Hertz between the two spectral maxima, is about 1.2 kHz and is close to the values reported previously for this cationic lipid with the identical deuteron labeling position, but in mixtures with POPC [22].

Adding OligoS or PolyA produces virtually no change in the quadrupolar splitting, either at 1:1 (middle spectra) or 2:1 (bottom spectra) anion/cation charge ratios. Similar results have been reported previously for the case of PolyA bound to DOTAP-γ-d_9/POPC mixtures [22]. There is an obvious decrease in the intensity at the center of these spectra upon adding nucleic acid chains, but this can be accounted for by the fact that the neutralized MLVs are much more readily concentrated than the highly charged MLVs. The concentration process removes any small vesicles and decreases the water content, both of which could otherwise contribute signal intensity at the isotropic frequency.

We conclude at this point that the cationic lipids retain virtually full mobility when complexed with an anionic polyelectrolyte. Under the same conditions the bound nucleotide chains are virtually immobilized, except for librations at the level of individual nucleotide segments.

3.4. ^{31}P-NMR of complexes of OligoS or PolyA with DOTAP/POPC mixtures

Fig. 5 contains ^{31}P-NMR spectra of complexes of mixed DOTAP/POPC (30/70) MLVs as a function of added OligoS (left hand column) or PolyA (right hand column). The top spectrum in each column is identical, and was obtained in the absence of nucleotide chains. Its line shape is characteristic of phospholipids in a liquid-crystalline lamellar bilayer architecture where the lipids experience rapid anisotropic motional averaging about their long molecular axes [31,32]. Consequently, the spectrum is motionally narrowed ($\Delta\sigma = \sigma_{33} - \sigma_{11} \approx 40$ ppm) and axially symmetric ($\eta = 0$).

As may be ascertained from the other spectra in Fig. 5, adding OligoS or PolyA does not alter the fundamental lamellar bilayer nature of the lipid assembly, since the ^{31}P-NMR spectrum of the phospholipids themselves changes little.

With increasing levels of added OligoS (left hand column), a narrow resonance line appears at the isotropic chemical shift of OligoS (approx. 56 ppm). This signal grows rapidly in intensity above the anion/cation equivalence point. We attribute this narrow resonance to free OligoS chains. A similar effect is observed with increasing levels of added PolyA, except the narrow resonance line appears only when the anion/cation ratio exceeds 2:1, and

the signal occurs at the isotropic chemical shift of PolyA (approx. 0 ppm).

Below the anion/cation equivalence point, however, there is only a broad, low intensity resonance signal at the isotropic chemical shift of OligoS. For PolyA, not even this broad signal is evident, although it might well be present but merely difficult to resolve when superimposed on the phospholipid's signal. Evidently, the bound nucleotide chains are not readily observed via ^{31}P-NMR without using cross-polarization techniques such as those used to obtain the spectra in Fig. 3.

These ^{31}P-NMR spectra confirm the findings of the UV-difference assay, in that signals correspond-

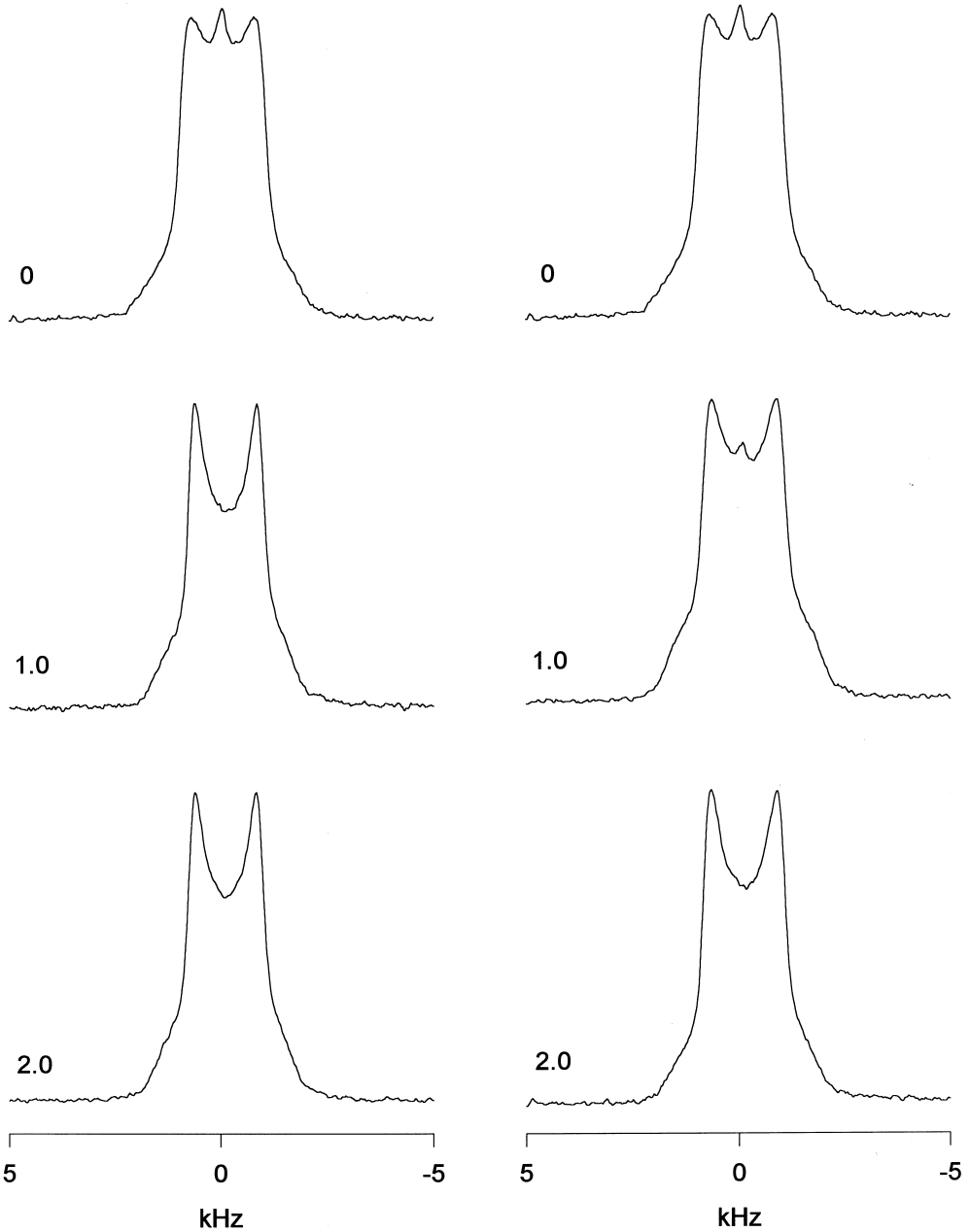

Fig. 4. ^{2}H-NMR spectra of fully hydrated 100% DOTAP-γ-d_3 mixed with OligoS (left hand column) or PolyA (right hand column). The top spectra were obtained in the absence of either OligoS or PolyA, the middle spectra at an anion/cation charge ratio of 1:1, and the bottom spectra at an anion/cation charge ratio of 2:1.

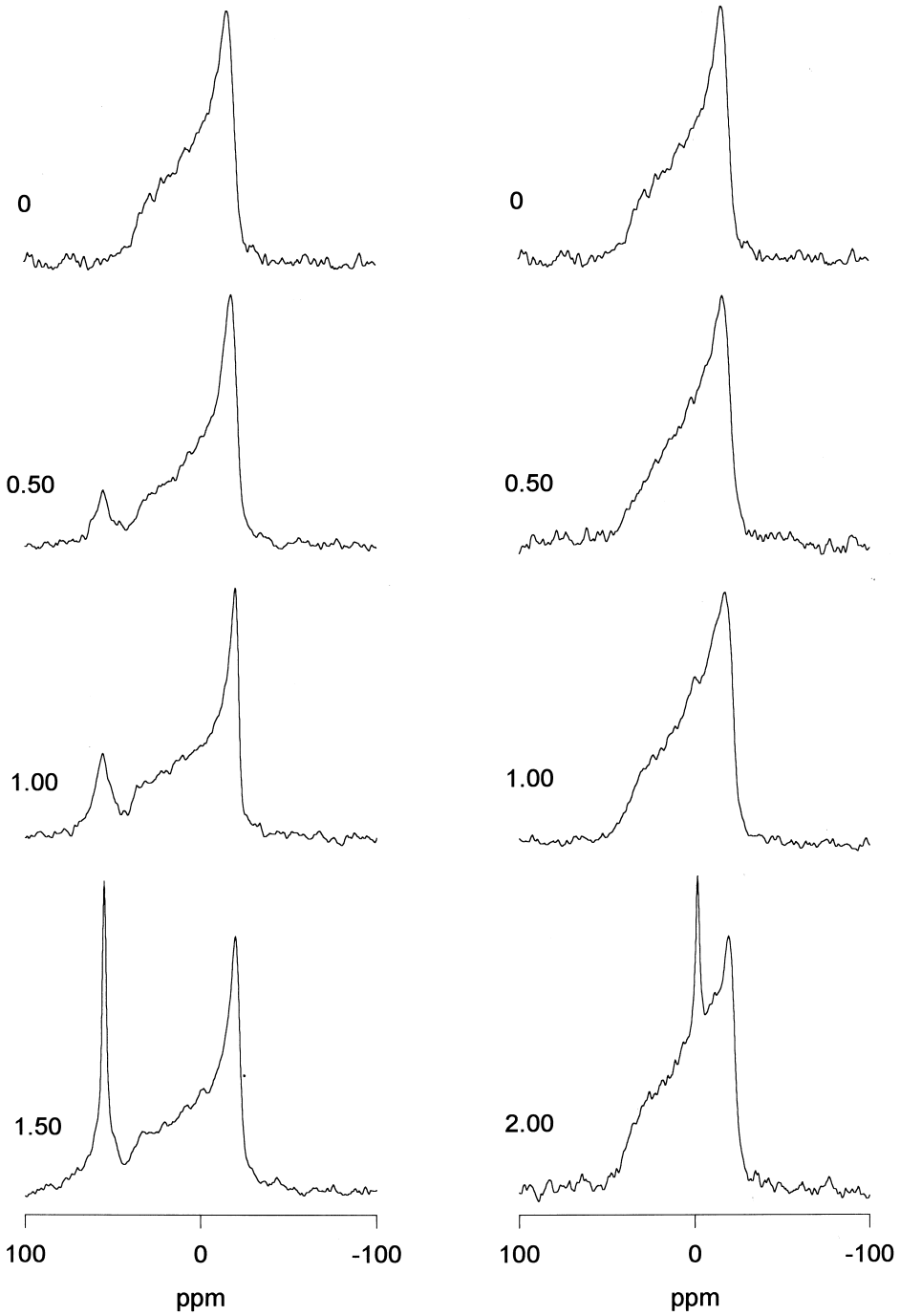

Fig. 5. ^{31}P-NMR spectra of mixed DOTAP/POPC (30/70) cationic MLVs as a function of added OligoS (left hand column) or PolyA (right hand column). The anion/cation ratio is indicated in the figure.

ing to free nucleotide chains only appear above the anion/cation equivalence point.

Can the ^{31}P-NMR resonance intensity of the free OligoS be related quantitatively to that of the phospholipid POPC? To address this point, ^{31}P-NMR spectra were acquired for OligoS added to 100% POPC MLVs, circumstances under which no OligoS binding should occur. It was found that the ratio of the integrated intensities of the OligoS versus POPC resonances was approx. 90% of that expected from

the known composition, i.e., within the error of the determination. Furthermore, the longitudinal relaxation times (T_1) of free OligoS and POPC were found to be similar, with values of 930 ms and 900 ms, respectively. Thus, any partial saturation of intensity due to too rapid repetition of the pulse sequence would be equivalent for both signals. To prove this, a spectrum was acquired with a relaxation delay sufficiently long as to permit complete relaxation (10 s). No change in the relative intensities of the OligoS and POPC resonances was observed. Finally, the transverse relaxation times (T_2) were likewise similar for OligoS and POPC (10 ms). Therefore, any differential T_2 relaxation during the τ delays of the Hahn echo pulse sequence would be minimal. We conclude that it is reasonable to approximate the amount of free OligoS by comparing its integrated signal intensity to that of POPC.

For the situation of OligoS added in an amount corresponding to an anion/cation ratio of 1.5:1 (Fig. 5, bottom spectrum, left hand column), the isotropic resonance at 56 ppm is only approx. 1/3 the intensity expected if no OligoS binding occurs. However, the narrow isotropic resonance of free OligoS cannot be separated from the broad underlying resonance observed at the same frequency below the equivalence point. At the equivalence point, the latter accounts for approx. 1/5 of the signal intensity expected if no OligoS binding occurs. Assuming, then, that no more than 1/5 of the bound OligoS contributes to the integrated signal intensity at the isotropic chemical shift, one calculates that at the anion/cation ratio of 1.5:1, there are 1.2 equivalents of OligoS bound, which agrees with the UV-difference assay results. Of course, one appreciates the approximate nature of this calculation, given the underlying assumptions.

In contrast to the case with OligoS, the amount of free PolyA cannot be quantified directly from the intensity of the isotropic resonance appearing at 0 ppm in the right hand column of spectra in Fig. 5. When this point was tested experimentally by adding PolyA to 100% POPC MLVs (ratio of 30/70 PolyA phosphorus/POPC phosphorus), the isotropic resonance due to free PolyA was only 1/3 the intensity expected, given that no PolyA binding should occur in the absence of cationic amphiphiles [25]. The T_1 and T_2 of the isotropic PolyA resonance and the bilayer POPC resonance were again roughly comparable, and could not be used to explain the loss of signal from PolyA. However, when a calibration experiment was performed relating the ^{31}P-NMR intensity of PolyA to its concentration in aqueous solution, i.e., in the absence of any amphiphiles, the relationship was non-linear, with the observed intensity falling off with increasing concentration, to the point of being almost 50% below the expected value at a concentration of 10 mg/ml. This is the concentration range pertinent to our studies. One possible explanation for this anomalous behavior is that DNA is known to form anisotropic phases at high concentrations [33]. Such circumstances would lead to line broadening and a differential intensity loss in the Hahn echo experiment used here. Regardless of the actual origin of this problem, it is obvious that one must exercise great care if one wishes more quantitative information from such spectra.

3.5. *UV-difference assay of ionic strength effects on OligoS or PolyA binding to DOTAP/POPC mixtures*

In a previous report we described the use of the UV-difference assay to examine the desorption of

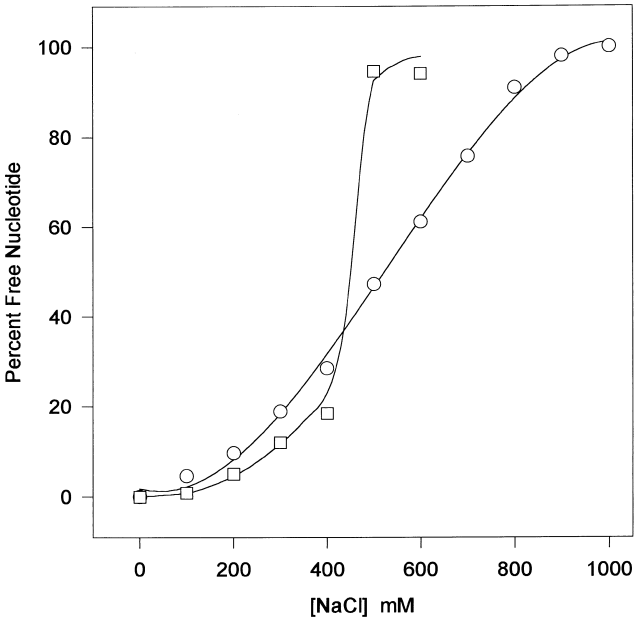

Fig. 6. UV-difference assay of the salt-induced desorption of OligoS (○) or PolyA (□) from DOTAP/POPC (30/70) mixtures. Each mixture contained a 1:1 nucleotide anion/DOTAP cation charge ratio. The PolyA data were originally reported in [22].

PolyA from DOTAP/POPC (30/70) mixtures as a function of ionic strength [22]. These results are reproduced in Fig. 6 along with new data for OligoS desorption from lipid mixtures of identical composition. In all samples, the ratio of nucleotide anion charge to amphiphilic cation charge was unity, i.e. overall charge neutrality. Fig. 6 shows that nucleotide chain desorption increases sigmoidally with increasing ionic strength, for both OligoS and PolyA. The added NaCl reduces the Coulombic attraction between the nucleotide chains and the cationic liposomes by a simple charge screening mechanism. The sigmoidal dependence of desorption is a manifestation of the cooperative nature of the electrostatic

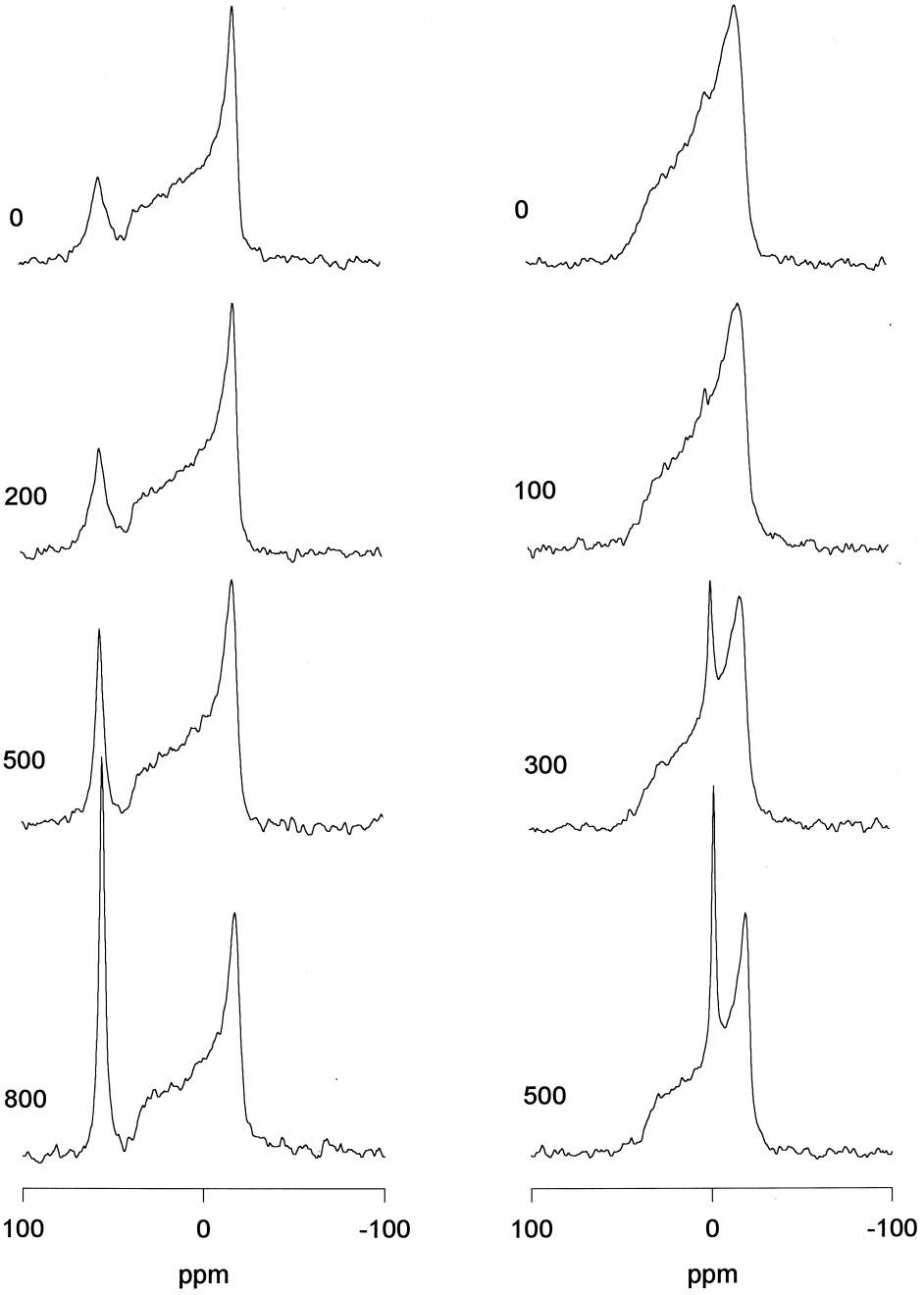

Fig. 7. ^{31}P-NMR monitoring of salt-induced desorption of OligoS (left hand column) and PolyA (right hand column) from DOTAP/POPC 30/70 mixtures. Each mixture contained a 1:1 anion/cation charge ratio. The NaCl concentration (mM) is shown in the figure.

binding of a multivalent molecule [34]. For instance, the multivalent cationic MARCKS protein desorbs from lipid bilayer surfaces containing 20 mole% acidic lipids at NaCl concentrations between 0.1 M and 0.5 M [35]. The ionic strength required to reduce the number of bound chains by one half is just over 400 mM for PolyA and just under 600 mM for OligoS. Note that at physiological ionic strengths the nucleotide chains remain bound to the cationic MLV surfaces.

There is a further clear difference in the salt-induced desorption of PolyA versus OligoS, in that PolyA shows a much steeper transition from bound to unbound states with increasing ionic strength, and the ultimate ionic strength required to achieve quantitative desorption is much lower.

3.6. ^{31}P-NMR and ionic strength effects on OligoS or PolyA binding to DOTAP/POPC mixtures

^{31}P-NMR spectra of OligoS (left hand column) and PolyA (right hand column) complexed with DOTAP/POPC (30/70) MLVs in a 1:1 anion/cation charge ratio are shown in Fig. 7 for the case of different ionic strengths of NaCl. The spectra indicate that under all conditions the lipids remain in a lamellar bilayer arrangement. With increasing ionic strength a narrow resonance appears at the isotropic chemical shift position of the corresponding nucleotide chain and grows progressively in intensity. We associate this resonance, again, with free OligoS or PolyA. For OligoS the intensity of the isotropic resonance no longer increases, i.e., desorption is complete, beyond a NaCl concentration of 800 mM. For PolyA the desorption is complete at a NaCl concentration of 500 mM. Therefore, the ^{31}P-NMR spectra confirm the conclusions drawn from the UV-difference assay regarding nucleotide chain desorption by salt.

The intensity of the isotropic OligoS resonance at 800 mM NaCl is 92% of that expected for the case of 100% desorption, based on a comparison with the integrated intensity of the POPC spectral envelope and the known global ratio of OligoS to POPC. For the case of PolyA, the difficulties in quantifying PolyA from its resonance intensity have been mentioned earlier. To circumvent this problem, a control sample was prepared containing only PolyA and POPC in the same ratios as in Fig. 7 and in the presence of 500 mM NaCl. Under these conditions one expects no PolyA binding. Using the relative intensities of the PolyA and POPC resonances in this sample as a benchmark, we deduce that for the case of DOTAP/POPC (30/70) MLVs in the presence of 500 mM salt, such as shown in Fig. 7, the PolyA is 100% desorbed. Hence, the ^{31}P-NMR data agree both qualitatively and quantitatively with the UV-difference assay results.

3.7. ^{31}P-NMR of DOPE/DOTAP and DOPE/CTAB mixtures

As a preliminary to investigating the effects of nucleotide chains on the architecture of cationic amphiphile+DOPE mixed vesicles, we examined ^{31}P-NMR spectra of DOPE mixed with either DOTAP or CTAB. The results are shown in Fig. 8.

The top ^{31}P-NMR spectra in Fig. 8 were obtained with 100% DOPE and are indicative of lipids in an inverted hexagonal H_{II} arrangement. Specifically, the spectra are reversed in sign relative to those of lipids in an L_α lamellar bilayer arrangement, with a low field shoulder and high field peak, and their residual chemical shift anisotropy is narrower by a factor of 2, i.e., $\Delta\sigma \approx 22$ ppm.

The spectra in the left hand column of Fig. 8 were obtained upon adding DOTAP to DOPE in the mole percent indicated. At 10 mole% DOTAP the mixture retains its overall hexagonal H_{II} architecture. At 20 mole% DOTAP the spectra show a superposition of hexagonal H_{II} and (probably) cubic (Q_{II}) phases, the latter being a high local curvature phase. At higher DOTAP levels a lamellar bilayer architecture is observed and dominates at 50 mole% DOTAP.

The spectra in the right hand column of Fig. 8 were obtained upon adding CTAB to DOPE in the mole percent indicated. With only 10 mole% CTAB the overall architecture converts completely to a lamellar bilayer. The line shape indicates some alignment of these vesicles in the magnetic field, a phenomenon observed elsewhere [36]. At 30 mole% CTAB, the mixture is obviously entirely lamellar bilayer in architecture, and no magnetic field induced orientation is observed. At 70 mole% CTAB the spectrum is dominated by an isotropic resonance.

The ability of cationically charged lipids to stabilize DOPE into a lamellar bilayer architecture has

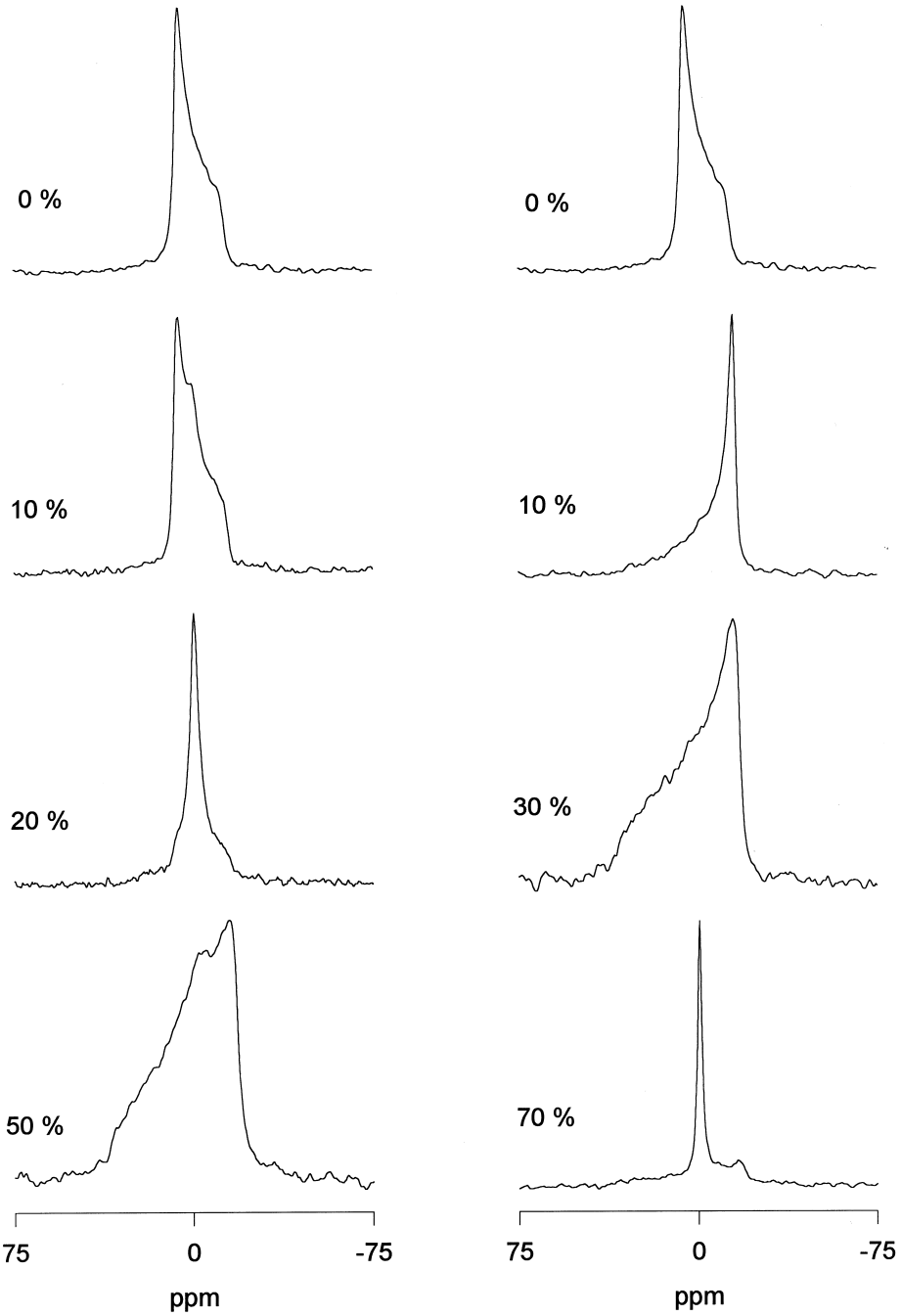

Fig. 8. ^{31}P-NMR spectra of DOPE mixed with various mole% DOTAP (left hand column) or CTAB (right hand column), as indicated in the figure.

been shown previously [9], and is reminiscent of similar behavior induced by anionically charged lipids [32].

We note, in addition, that POPC mixed with DOTAP forms lamellar bilayers at all ratios [25], while mixing POPC with CTAB produces a lamellar-type ^{31}P-NMR spectrum at CTAB mole fractions up to 0.5 (data not shown).

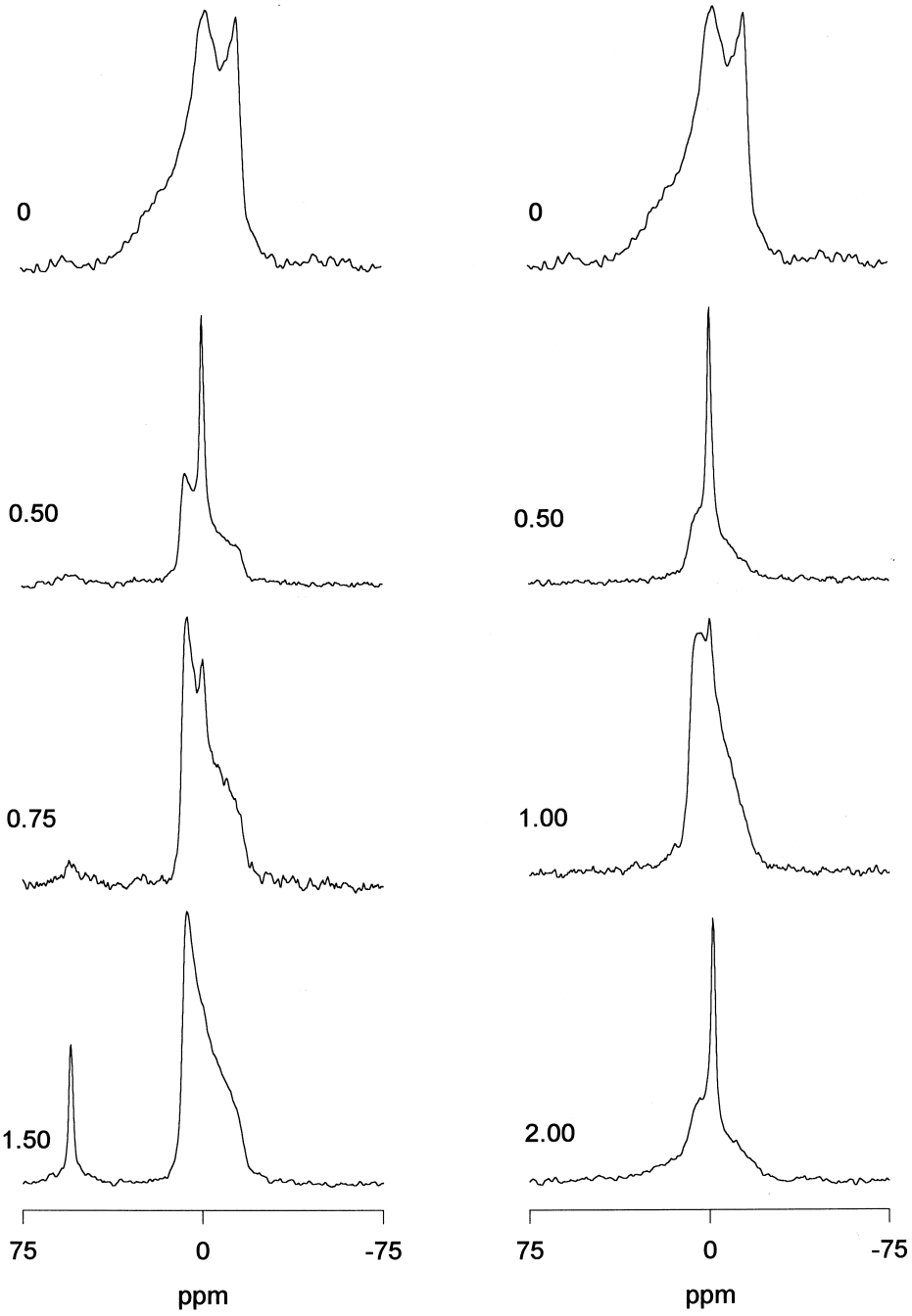

Fig. 9. ^{31}P-NMR spectra of DOTAP/DOPE 30/70 mixtures as a function of added OligoS (left hand column) or PolyA (right hand column) at the indicated anion/cation charge ratio.

3.8. *Effects of OligoS and PolyA on the morphology of DOTAP/DOPE (30/70) mixtures*

In the absence of either OligoS or PolyA, mixtures of DOTAP/DOPE (30/70) produce predominantly lamellar bilayer-type ^{31}P-NMR spectra, as shown in the top row of Fig. 9. There is, however, a significant fraction of broad isotropic signal present. Adding OligoS produces a conversion to a predominantly hexagonal H_{II}-type ^{31}P-NMR spectrum, with a residue of narrow isotropic signal, as shown in the left hand column of spectra in Fig. 9. The isotropic sig-

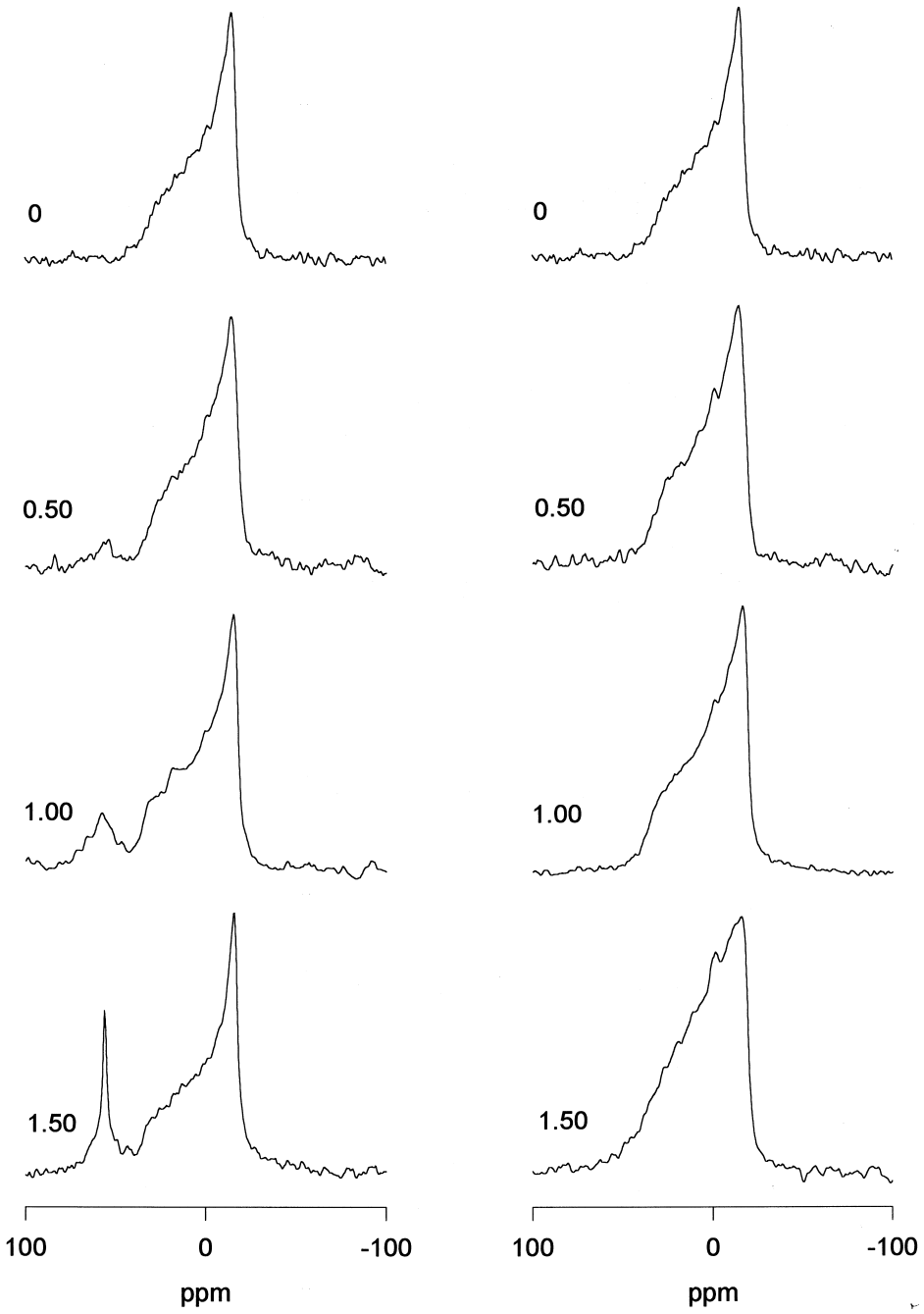

Fig. 10. ^{31}P-NMR spectra of CTAB/DOPE 30/70 mixtures as a function of added OligoS (left hand column) or PolyA (right hand column) at the indicated anion/cation charge ratio.

nal disappears as more OligoS is added. When excess OligoS is present, a narrow resonance appears at the isotropic chemical shift position of OligoS, and the phospholipid signal indicates a total conversion to the hexagonal H_{II} architecture.

As shown in the right hand column of spectra in Fig. 9, when PolyA is added to the DOTAP/DOPE (30/70) mixtures one observes an analogous conversion to a predominantly hexagonal H_{II} architecture, through an intermediate isotropic phase, with excess free PolyA appearing at its expected isotropic resonance position.

These results demonstrate that complexing nucleotide chains with DOTAP/DOPE mixtures causes a conversion to the hexagonal H_{II} architecture. Fig. 9 indicates that, in general, PolyA is considerably less effective in this regard than OligoS.

A further point regarding the spectra in Fig. 9 concerns the resonance for OligoS at 56 ppm. In Fig. 5, for the case of DOTAP/POPC (30/70) mixtures, a broad resonance was readily observed at this frequency at anion/cation ratios well below the equivalence point, i.e., when all OligoS should be bound. In Fig. 9, however, there is very little evidence of this same resonance.

3.9. Effects of OligoS and PolyA on the morphology of CTAB/DOPE (30/70) mixtures

Fig. 10 shows a series of ^{31}P-NMR spectra of CTAB/DOPE (30/70) mixtures to which have been added either OligoS (left hand column) or PolyA (right hand column) in the indicated anion/cation charge ratios. At 30 mole% CTAB causes a complete conversion to a lamellar bilayer architecture as obvious from the top spectra in the figure, and as expected given the results shown in Fig. 8. Adding either OligoS or PolyA fails to change the architecture of the lipid mixtures, which remain lamellar bilayers at all charge ratios. Binding of the nucleotide chains to these cationic surfaces certainly occurs, since free nucleotide chains do not appear in the spectra until the concentration exceeds the anion/cation equivalence point.

Evidently, charge neutralization is not a sufficient condition to induce non-bilayer phases in CTAB/DOPE mixtures.

3.10. Effects of ionic strength on OligoS binding to DOPE/DOTAP and DOPE/CTAB mixtures

The effects of increasing ionic strength on the binding of OligoS, added in a 1:1 anion/cation charge ratio, to mixtures of CTAB/DOPE 30/70 and DOTAP/DOPE 30/70 likewise was followed via ^{31}P-NMR (data not shown). Increasing ionic strength produced desorption of the OligoS from either lipid mixture, as evident by the appearance of a narrow isotropic resonance at a chemical shift of 56 ppm. For the CTAB/DOPE mixtures, the DOPE yielded a bilayer-type ^{31}P-NMR line shape at all salt concentrations. For the DOTAP/DOPE mixtures, the DOPE yielded an inverted hexagonal H_{II} line shape at all salt concentrations. Hence, there is no reversion from the OligoS-induced hexagonal H_{II} phase back to the original bilayer L_α phase simply because OligoS desorbs. This indicates that NaCl and OligoS are equally capable of inducing this change in the morphology of the lipid assembly.

4. Discussion

Vastly greater efficiencies of gene transfer are achieved when DNA is packaged with cationic amphiphiles, and when the overall assembly takes on a non-bilayer, as opposed to a bilayer, arrangement [5,9]. The goal of the present study was to investigate the factors contributing to morphological changes in complexes of nucleotide chains with cationic amphiphiles plus helper lipids using ^{31}P-NMR as the investigative tool. We find that all three components exert an influence on the final morphology, in addition to external factors such as ionic strength.

4.1. Nucleotide chain length effects

When there is excess cationic charge from cationic amphiphiles, nucleotide chains bind to lipid bilayer surfaces with a 1:1 anion/cation stoichiometry, indicating that they must lie flat along the surface of the lipid bilayer [25]. The result is a virtual immobilization of the nucleotide chains at the surface, such that their ^{31}P-NMR spectra consist of broad powder patterns, resembling those of dry powders of nucleotide chains. In fact, such spectra can only be observed using cross-polarization techniques to enhance sensitivity and signal-to-noise, as shown in Fig. 3. Without cross-polarization, the signal intensities of the immobilized nucleotide chains are weak, and their longitudinal (T_1) relaxation times are long, particularly with respect to those of the mobile phospholipids. Under ordinary spectral acquisition conditions, like the Hahn echo technique used to acquire the spectra in Fig. 5, the immobilized nucleotide chains become NMR invisible.

Nevertheless, the ^{31}P-NMR spectra in Fig. 3 indicate that the longer PolyA chain ($n \approx 18\,000$) experi-

ences greater segmental flexibility than the shorter OligoS chain ($n=21$) as the charge equivalence point is approached. This may be attributed to entanglement effects associated with PolyA's greater length, and the consequent difficulty of lying down flat on a surface.

When there is excess anionic charge from nucleotide chains versus cationic charge from surface amphiphiles, free nucleotide chains begin to appear in solution, as detected with either UV (Fig. 3) or ^{31}P-NMR (Fig. 5). This begins to occur at an anion/cation charge ratio of 1:1 for OligoS, but not until 2:1 for PolyA.

This particular difference in the behavior of OligoS versus PolyA may be attributed to the greater conformational flexibility of the longer PolyA chain. Polynucleotides are relatively stiff polymers and the notion of the chain persistence length becomes useful. This is a measure of the tendency of successive chain segments to continue in the direction dictated by prior segments. If the chain is short relative to the persistence length, then it behaves essentially as a rigid rod. If the chain is long relative to the persistence length, then it retains considerable flexibility and behaves more like a random coil polymer. The persistence length of double-stranded DNA is greater than 50 nm, corresponding to approx. 150 base pairs [33]. Single-stranded nucleotide chains such as those employed here will have shorter persistence lengths, but it is clear that OligoS must be considered more like a rigid rod while PolyA, being many times longer than the persistence length, will enjoy greater overall conformational flexibility. Consequently, above the equivalence point, where not every nucleotide phosphate can be paired with a cationic amphiphile, PolyA is capable of adopting a 'brush-like' conformation which maximizes the number of PolyA chains bound. As binding levels increase, the number of anion/cation pairs per PolyA chain decreases and surface crowding increases. Further binding ceases when the favorable Coulombic attractions are overbalanced by the unfavorable entropic cost of conformational adaption. OligoS, on the other hand, cannot readily adapt conformationally and so reaches this balance point much sooner.

This difference in behavior as a function of size may be important for understanding differences in gene transfection efficiencies. Longer nucleotide chains have been shown to have reduced entrapment efficiencies in vesicles [18], as well as reduced efficiencies of gene transfection [19]. The results presented here indicate that longer nucleotide chains have difficulty achieving 1:1 charge pairing with cationic amphiphiles and form a rougher, thicker coating at the lipid bilayer surface. This could lead to vesicle entrapment difficulties and, possibly, to regions of the surface having a net anionic charge, despite the complex's overall cationic charge. An overall cationic charge encourages electrostatic attraction to generally anionically charged target cell membrane.

4.2. Helper lipid effects

When the zwitterionic, or helper, lipid is POPC, the complexes formed with nucleotide chains and cationic lipids always take on a lamellar L_α lipid bilayer arrangement, as diagnosed by ^{31}P-NMR. This is true regardless of the details of nucleotide chain length, or cationic lipid structure, or ionic strength. However, another zwitterionic lipid, DOPE, is commonly included in transfection formulations in order to increase the efficiency of transfection. The enhancement is believed to arise from the preference of DOPE to assume an inverted hexagonal H_{II}, rather than a lamellar L_α, architecture. This destabilizing influence of DOPE on lipid bilayer permeability lowers the energy barrier to transfer of DNA across the target cell membrane.

This property of DOPE is manifest in the changing architecture of the lipid self-assembly when DOPE is mixed with the cationic amphiphile DOTAP, as reported by the ^{31}P-NMR spectra in Fig. 8. DOPE alone prefers an inverted hexagonal H_{II} architecture. In terms of the 'shape' model of Israelachvili [37,38], this tendency of DOPE is a result of its overall inverted cone shape. This is a consequence of DOPE's combination of a small head group with unsaturated acyl chains [32]. POPC, in contrast, possesses a larger head group, which confers an overall cylindrical shape and, therefore, a preference to assemble into a lamellar bilayer architecture. When DOPE is mixed with DOTAP, which by itself prefers a lamellar bilayer architecture, eventually DOTAP prevails and the mixture converts from a hexagonal H_{II} to a lamellar L_α architecture.

OligoS or PolyA binding to DOPE/DOTAP mix-

tures causes a reversion to the hexagonal H_{II} architecture, as reported in the ^{31}P-NMR spectra in Fig. 9, because electrostatic repulsion between individual DOTAP molecules is a significant contributor to the effective size of the DOTAP head group. Once this charge repulsion is reduced by electrostatic coupling to OligoS or PolyA, DOTAP effectively changes shape and the entire complex can adopt a hexagonal H_{II} arrangement.

The conversion to the hexagonal H_{II} architecture in DOPE/DOTAP mixtures is more readily induced by OligoS than by PolyA. This may have to do, again, with entanglement effects, i.e. the difficulty of the large PolyA chain to bring all its charges to bear on the surface. On the other hand, it may also be that it is more difficult to pack the large PolyA chains into the confines of the aqueous tubes characteristic of the hexagonal H_{II} phase, relative to the shorter OligoS chains. Certainly, the ^{31}P-NMR spectral line shapes are less well defined in the case of PolyA than for OligoS.

4.3. Cationic lipid effects

When DOPE is mixed with CTAB, which by itself prefers a micellar architecture, a lamellar architecture is immediately preferred even at low CTAB molar ratios. This is because CTAB, with its single alkyl chain and large cationic head group, possesses a cone shape complimentary to the inverted cone shape of DOPE. At high CTAB molar ratios, its preference for a micellar architecture dominates.

OligoS or PolyA binding to DOPE/CTAB mixtures causes no reversion to the hexagonal H_{II} architecture of the kind observed in DOPE/DOTAP mixtures, as reported in the ^{31}P-NMR spectra in Fig. 10. One reasons that the electrostatic repulsion between individual CTAB molecules is a less significant contributor to the effective size of the CTAB head group than is the case with DOTAP. Therefore, even eliminating the CTAB-CTAB charge repulsion by electrostatic coupling to OligoS or PolyA does not change the effective overall shape of CTAB, and the mixture retains a lamellar L_{α} architecture.

The significance of this finding for the design of effective gene transfection formulations is that certain cationic amphiphiles will permit a change in the architecture of the complexes of nucleotide chains with cationic lipids plus helper lipids, while others will not. Gene transfection is believed to occur through a destabilization of either the cell's plasma membrane if direct fusion occurs, or the endosomal membrane if the effective mechanism is endocytotic. In either case, the ability of DOPE to form non-bilayer phases is an important aspect of enhancement in transfection efficiencies [14,39]. For instance, it has been shown that replacing DOPE with DOPC results in packages which are inefficient in promoting transfection. It is equally clear from the results reported here that the structure of the cationic lipid influences, even dictates, the ability of DOPE to precipitate a non-bilayer architecture.

4.4. Ionic strength effects

Increasing ionic strength screens the electrostatic attraction between nucleotide chains and oppositely charged lipids. The result is desorption of nucleotide chains from lipid bilayer surfaces, as indicated by the UV and ^{31}P-NMR results in Figs. 6 and 7, respectively. Importantly, chain desorption occurs only at ionic strengths far exceeding physiological levels.

A higher ionic strength is required to desorb OligoS than PolyA for the case of a global 1:1 anion/cation ratio. This indicates that OligoS is held more tightly at the lipid bilayer surface and must have a greater proportion of its anionic charges paired electrostatically with cationic charges. Therefore, the ionic strength effects on nucleotide chain binding confirm our earlier conclusion that OligoS tends to lie down flat on the bilayer surface while PolyA adopts a more brush-like conformation. High ionic strength will also reduce intersegment charge repulsion, thereby encouraging a more compact polyelectrolyte chain conformation. This will tend to favor the unbound state entropically. Such effects will have less influence on the short chain of OligoS, thereby leading to differences in its salt desorption behavior relative to PolyA.

The most general principle that arises from this work is that if one wishes to correlate the efficiency of transfection with the morphology of the mixture of polynucleotide+cationic amphiphile+helper lipid, one may make morphological predictions based on known principles governing such matters, but it is essential to characterize a particular mixture experi-

mentally, given the complexities of the various interactions which will be present.

Acknowledgements

This work was supported by a Natural Sciences and Engineering Research Council (NSERC) of Canada research grant (P.M.M.). The authors wish to thank ISIS Pharmaceuticals for the kind gift of OligoS.

References

[1] R. Leventis, J.R. Silvius, Biochim. Biophys. Acta 1023 (1990) 124–132.
[2] J. Zabner, A.J. Fasbender, T. Moninger, K.A. Poellinger, M.J. Welsh, J. Biol. Chem. 270 (1995) 18997–19007.
[3] D.S. Friend, D. Papahadjopoulos, R.J. Debs, Biochim. Biophys. Acta 1278 (1996) 41–50.
[4] H. Gershon, R. Ghirlando, S.B. Guttman, A. Minsky, Biochemistry 32 (1993) 7143–7151.
[5] B. Sternberg, F.L. Sorgi, L. Huang, FEBS Lett. 356 (1994) 361–366.
[6] J. Gustafsson, G. Arvidson, G. Karlsson, M. Almgren, Biochim. Biophys. Acta 1235 (1995) 305–312.
[7] N. Dan, Biophys. J. 71 (1996) 1267–1272.
[8] J.O. Radler, I. Koltover, T. Salditt, C.R. Safinya, Science 275 (1997) 810–814.
[9] K.W.C. Mok, P.R. Cullis, Biophys. J. 73 (1997) 2534–2545.
[10] D. Lasic, H. Strey, M.C.A. Stuart, R. Podgornik, P.M. Frederik, J. Am. Chem. Soc. 119 (1997) 832–833.
[11] D. Harries, S. May, W.M. Gelbart, A. Ben-Shaul, Biophys. J. 75 (1998) 159–173.
[12] B.J. Battersby, R. Grimm, S. Huebner, G. Cevc, Biochim. Biophys. Acta 1372 (1998) 379–383.
[13] J.H. Felgner, R. Kumar, C.N. Sridhar, C.J. Wheeler, Y.J. Tsai, R. Border, P. Ramsey, M. Martin, P.L. Felgner, J. Biol. Chem. 269 (1994) 2550–2561.
[14] H. Farhood, N. Serbina, L. Huang, Biochim. Biophys. Acta 1235 (1995) 289–295.
[15] H. Farhood, R. Bottega, R.M. Epand, L. Huang, Biochim. Biophys. Acta 1111 (1992) 39–246.
[16] N.J. Egilmez, Y. Iwanuma, R.B. Bankert, Biochem. Biophys. Res. Commun. 221 (1996) 169–173.
[17] H.M. Deshmukh, L. Huang, New J. Chem. 21 (1997) 113–124.
[18] P.-A. Monnard, T. Oberholzer, P.L. Luisi, Biochim. Biophys. Acta 1329 (1997) 39–50.
[19] I. van der Woude, H.W. Visser, M.B.A. ter Beest, A. Wagenaar, M.H.J. Ruiters, J.B.F.N. Engberts, D. Hoekstra, Biochim. Biophys. Acta 1240 (1995) 34–40.
[20] B. Sternberg, J. Liposome Res. 6 (1996) 515–533.
[21] Y.S. Tarahovsky, R.S. Khusainova, A.V. Gorelov, T.I. Nicolaeva, A.A. Deev, A.K. Dawson, G.R. Ivanitsky, FEBS Lett. 390 (1996) 133–136.
[22] P. Mitrakos, P.M. Macdonald, Biochim. Biophys. Acta 1374 (1998) 21–33.
[23] M. Rance, R.A. Byrd, J. Magn. Reson. 52 (1983) 221–240.
[24] J.H. Davis, K.R. Jeffrey, M. Bloom, M.I. Valic, T.P. Higgs, Chem. Phys. Lett. 42 (1976) 390–394.
[25] P. Mitrakos, P.M. Macdonald, Biochemistry 35 (1996) 16714–16722.
[26] N.J. Zuidam, Y. Barenholz, Biochim. Biophys. Acta 1368 (1998) 115–128.
[27] S.J. Eastman, C. Siegel, J. Tousignant, A.E. Smith, S.H. Cheng, R.K. Scheule, Biochim. Biophys. Acta 1325 (1997) 41–62.
[28] K.J. Crowell, P.M. Macdonald, J. Phys. Chem. B 101 (1997) 1105–1109.
[29] K.J. Crowell, P.M. Macdonald, J. Phys. Chem. B 102 (1998) 9091–9100.
[30] P. Mitrakos, P.M. Macdonald, Biochemistry 36 (1997) 13647–13656.
[31] P.R. Cullis, B. de Kruijff, Biochim. Biophys. Acta 559 (1979) 399–420.
[32] J. Seelig, Biochim. Biophys. Acta 515 (1978) 105–140.
[33] K. Merchant, R.L. Rill, Biophys. J. 73 (1997) 3154–3163.
[34] C.A. Buser, J. Kim, S. McLaughlin, R.M. Peitzsch, Mol. Membr. Biol. 12 (1995) 69–75.
[35] J. Kim, T. Shishido, X. Jiang, A. Aderem, S. McLaughlin, J. Biol. Chem. 269 (1994) 28214–28219.
[36] J. Seelig, F. Borle, T.A. Cross, Biochim. Biophys. Acta 814 (1985) 195–198.
[37] J.N. Israelachvili, D.J. Mitchell, Biochim. Biophys. Acta 389 (1975) 13–19.
[38] J.N. Israelachvili, Biochim. Biophys. Acta 469 (1977) 221–225.
[39] I. Wrobel, D. Collins, Biochim. Biophys. Acta 1235 (1995) 296–304.